CFD SIMULATION OF COMBUSTIÓN IN A D.I DIESEL ENGINE

Alvaro Delgado Mejía*, John Agudelo Santamaría, Elkin Gutiérrez Velásquez

Universidad de Antioquia, Medellín, Colombia. Calle 67 # 53 - 108

*Tel (57 4) 219 85 47, adelgado@udea.edu.co

ABSTRACT

This paper presents a comparative study of the combustion process in a direct injection diesel engine. For this, a numerical simulation using the CFD (Computational fluid dynamics) code OpenFoam, of the compression, injection, evaporation, ignition and combustion of a direct injection diesel engine was carried out. The results have been contrasted with experimental data obtained in a diesel test bench for several operational conditions, which has been treated by means of a thermodynamic model of one zone. The comparison was made in terms of characteristic parameters that describe the diesel combustion, as the temporal variation of pressure, temperature, heat release rate inside the combustion chamber and the gaseous emissions.

It was found that the simulated pressure match very well the pressure measured in all cases analyzed, though the temperature profiles and heat release have some difference, possibly because of mismatches in the characteristics of injection and the combustion model used in the simulation. The results demonstrate the benefits and the ability of CFD tools applied to the analysis of combustion in diesel engines.

1.- Introduction

Nowadays automotive industry is facing a big challenge respecting the fulfillment of the harmful emission normative, like nitrogen oxides and particulates in the case of diesel engines. In the goal of this objective, different solutions have been considered, being

simulation one of the most developed in the last years. In this sense, multidimensional combustion simulation has been improved by the proposal of different models for liquid injection, atomization, evaporation, heat transfer, ignition and combustion, making possible their inclusion in some commercial simulation codes, although it is evident that other aspects like turbulence modeling and mesh size must be optimized [1]. However, the development of such tools represent a step forward in the design and optimization of combustion engines, to the point that such computational tools have changed the way researchers conceive the phenomenology of these processes.

At this point, computational fluid dynamics has become an indispensable tool for designers, because it gives them the opportunity to gain valuable information about engine performance for several operating scenarios. Although the degree of development of these tools has been remarkable, it is also true that it has been directly related to the advance in computer systems, so there still are certain limitations in their applicability, mainly for reasons of time processing.

Despite the phenomenon of combustion in a diesel engine is extremely complex as it is characterized by their transient, multiphase, chemically reactive and highly turbulent nature, it has been subject of numerous studies that have contributed to their understanding and suitable modeling. Early works in simulating combustion processes are attributed to those made by the working group of Los Alamos National Laboratory (LANL) [2, 3, 4], with Von Newman in the lead, who propos the first computer models combustion to be solved by numerical calculations, and the methods of stability that now constitute the basis for the analysis of linear systems of partial differential equations. Later, based on the work of LANL, Spalding et al [5] gave the first steps in building a CFD simulation of combustion, resulting in codes that were later adopted by most commercial CFD codes available today. In the decade of the 90's LES methods (Large Eddy Simulation) were developed for reactive flows, which could be applied to turbulent flows in complex geometries, being an improvement over the RANS methods (Reynolds Average Navier Stokes) because the perturbations (vortices) on a large scale can already be modeled. LES methods also allow not only more precise estimates, but it offers the possibility to analyze

the interactions between combustion and acoustics, giving rise to an interest of the industry to solve the problems of combustion instability [6]. Present efforts are aimed to reach a spatial resolution that allows the direct numerical simulation (DNS) and introduce kinetic detailed chemical schemes, although flames in very simple geometries have been calculated with this technique [5].

2.- Conditions for the simulation

On a direct injection diesel engine mounted on a test bench (Table I), several tests at variable speed and load were carried out, in order to characterize its mechanical and environmental performance when it was fed with commercial diesel fuel and mixtures of palm oil biodiesel. Thus, the pressure inside the combustion chamber was measured by means of a piezoelectric transducer, as the mass flows of air and fuel, the temperatures of lubricating oil, inlet air and exhaust gas and gaseous emissions concentration of O_2, CO, CO_2, HC and NOx. Only four conditions of functioning were selected to be simulated numerically, characterized for the same angular velocity of 2000 rpm and loads of 20 Nm, 40 Nm, 60 Nm and 80Nm (Table II).

Tabla I. Technical specifications of the engine used in the tests

Referencia	**ISUZU 4JA1**
Type	Diesel direct Injection
Feeding	Turbocharged
Displacement	2499 cm^3
Configuration	4 cylinders in line
Bore / Stroke	93 mm / 92 mm
Compresión ratio	18.4:1
Power	59 kW (80 hp) @ 4100 rpm
Torque	170 Nm @ 2300 rpm
Inyection pump	Mechanical rotative

Tabla II. Conditions of functioning that were simulated

	Simulation #1	**Simulation #2**	**Simulation #3**	**Simulation #4**
Load (Nm)	20	40	60	80

Initial Pressure (kPa)	103	110	112	118
Initial Temperature (K)	321	325	328	334
Injected fuel mass (mg)	2.02	2.81	3.54	4.40
Start of injection (º)	-23	-24	-25	-28
Duration of injection (º)	15	15	15	15

The model on which the simulations were carried out consisted in one quarter of the engine combustion chamber in which the experiments were conducted, and it was formed with about 250 000 computational cells (Figure 1), on which the governing equations were solved [7].

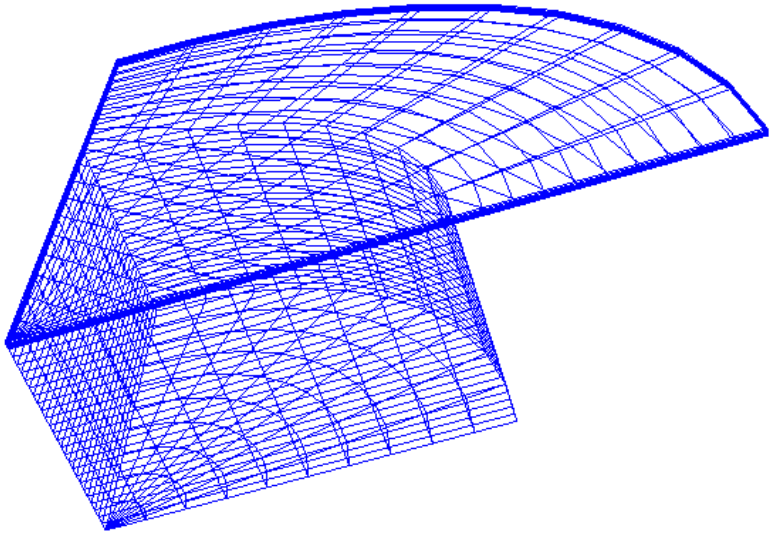

Figure 1, Geometrical model of the combustion chamber used in the simulation, with its meshing

Continuity equation

The continuity equation, or rather species transport equation, for one component in a multicomponent mixture reads:

$$\frac{\partial \rho_m}{\partial t} + \nabla \cdot (\rho_m \mathbf{u}) = \nabla \cdot \left[\rho D \nabla \left(\frac{\rho_m}{\rho} \right) \right] + f_m + \dot{\rho}^{s_m} \delta_{ml}$$

Where ρ_m (kg/m^3) is the mass density of specie *m*, ρ (kg/m^3) the total gaseous mass density, **u** (m/s) the gas velocity, f_m (kg/m^3 s) the source/sink term due to chemistry and ρ_m^s (kg/m^3 s) the source due the evaporation of liquid.

Momentum equation

The averaged momentum equation for the gas reads:

$$\frac{\partial(\rho u)}{\partial t} + \nabla \cdot (\rho \mathbf{u}\mathbf{u}) = -\nabla p + \nabla \cdot \sigma + F_s + \rho\, g - \frac{2}{3}\nabla(\rho k)$$

Where p is the gas pressure (Pa), σ the viscous stress tensor (N/m^2), Fs is the rate of gain / loss of momentum per unit of volume due to spray (N/m^3 s) and g is the body force, assumed as constant.

Energy equation

The internal energy equation reads:

$$\frac{\partial(\rho e)}{\partial t} + \nabla \cdot (\rho \mathbf{u} e) = -\, p\nabla \cdot \mathbf{u} - \nabla \cdot \mathbf{J} + \dot{Q}^c + \dot{Q}^s$$

Where e is the specific internal energy (J/kg) and **J** (W/m^2) is the heat flux vector, which is the sum of heat conduction and enthalpy diffusion. Q^c y Q^s (J/m^3 s) are the source terms due to the chemical heat release and spray interaction, respectively.

Turbulence equations

Among the turbulence models of the RANS type (Reynolds averaged numerical simulation), the most popular are the standard k-ε, the RNG k-ε, the realizable k-ε and Reynolds stress model (RSM). In all of them ε (m^2/s^2) and k (m^2/s^2) refer respectively to the turbulent kinetic energy and their dissipation rate. In the present work it has been chosen the k-ε model, because of its robustness, its simplicity and reasonable accuracy.

$$\frac{\partial(\rho k)}{\partial t} + \nabla \cdot (\rho \mathbf{u} k) = -\frac{2}{3}\rho k \nabla \cdot \mathbf{u} + \sigma : \nabla \mathbf{u} + \nabla \cdot \left[\left(\frac{\mu}{\mathrm{Pr}_k} \right) \nabla k \right] + \rho\varepsilon + \frac{\partial k}{\partial t}$$

$$\frac{\partial(\rho \varepsilon)}{\partial t} + \nabla \cdot (\rho \mathbf{u} \varepsilon) = -\left(\frac{2}{3} C_{\varepsilon 1} - C_{\varepsilon 3} \right) \rho\varepsilon \nabla \cdot \mathbf{u} + \nabla \cdot \left[\left(\frac{\mu}{\mathrm{Pr}_\varepsilon} \right) \nabla \varepsilon \right]$$

$$+ \frac{\varepsilon}{k} C_{\varepsilon 1} \sigma : \nabla \mathbf{u} - C_{\varepsilon 2} \rho\varepsilon + C_s \frac{\partial k}{\partial t}$$

Pr is the Prandtl number and μ the gaseous dynamic viscosity (kg/m s). The value of the constants are *Cs* 1.5, $C_{\varepsilon 1}$ is 1.44, $C_{\varepsilon 2}$ 1.92 and $C_{\varepsilon 3}$ 1.5, according to reference [7].

The simulation of diesel combustion has been developed with an open source CFD code, called OpenFoam, which is based on the finite element method to solve the transport equations governing the flow. Given that the process in question involves a two-phase fluid medium, one corresponding to the intaking air during the admission, and another for liquid fuel injection, it has been used an Eulerian scheme for the first phase and a Lagrangian for the liquid phase, as it has been done in various works treating on numerical simulation of diesel combustion [5].

In this work different models for the atomization, secondary breakup, evaporation, ignition and combustion have been taken in account, their formulation and validation is detailed in references [8, 9], however in Table III are listed the models used.

Tabla III. Models used in the numerical simulation

Phenomenon	**Model**
Atomization	LISA
Secundary break up	KHRT
Evaporation	Standar
Heat transfer	Ranz - Marshall
Ignition	Shell
Combustión	PaSR (Partially Steerred Reactor)
NOx	Extended Zeldovich

Each simulation comprised the compression and expansion strokes, in which the system can be assumed as thermodynamically closed. The fuel used in the simulation was the n-heptane (C_7H_{16}) which is usually used as a surrogate for the diesel fuel, because of their ease of ignition [10], while in the modeling of gaseous emissions it has been used a reduced scheme consisting in 15 species and 39 reactions (Figure 2).

CO	+ O	+ M	= CO2	+ M	H	+ O	+ M	= OH	+ M
CO	+ OH		= CO2	+ H	H	+ H	+ H2O	= H2	+ H2O
CO	+ O2		= CO2	+ O	H	+ H	+ CO2	= H2	+ CO2
HO2	+ CO		= CO2	+ OH	H	+ OH	+ M	= H2O	+ M
H2	+ O2		= OH	+ OH	H	+ O	+ M	= OH	+ M
H2	+ OH		= H2O	+ H	O	+ O	+ M	= O2	+ M
O	+ OH		= O2	+ H	H	+ HO2		= H2	+ O2
O	+ H2		= OH	+ H	HO2	+ HO2		= H2O2	+ O2
H	+ HO2		= O	+ H2O	OH	+ OH	(+M)	= H2O2	(+M)
O	+ OH	+ M	= HO2	+ M	H2O2	+ H		= HO2	+ H2
H	+ O2	+ M	= HO2	+ M	H2O2	+ OH		= H2O	+ HO2
H	+ O2	+ O2	= HO2	+ O2	H2O2	+ H		= H2O	+ OH
H	+ O2	+ H2O	= HO2	+ H2O	H2O2	+ O		= H2O	+ O2
H	+ O2	+ N2	= HO2	+ N2	H2O2	+ O		= OH	+ HO2
OH	+ HO2		= H2O	+ O2	H2	+ HO2		= H2O	+ OH
H	+ HO2		= OH	+ OH	CO2	+ N		= NO	+ CO
O	+ HO2		= O2	+ OH	N	+ NO		= N2	+ O
OH	+ OH		= O	+ H2O	N	+ O2		= NO	+ O
H	+ H	+ M	= H2	+ M	N	+ OH		= NO	+ H
H	+ H	+ H2	= H2	+ H2					

Figure 2, scheme of reactions employed in the CFD simulation

3.- Results and discussion

Since a three-dimensional simulation only solves numerically the set of partial differential equations governing the problem in question, the results consist of the history over time of the variables involved in the analysis, for each control volume or computational cell mesh, which occupies a position in space. However, the experimental measurements, such as the pressure inside the combustion chamber, are those corresponding to a spatial average, since the sensor is not capable of discretizing the measurement by zones. For this reason, the

simulation results presented below represent spatial averages of most representing variables in the process of combustion.

In Figure 3, the pressure obtained by the CFD simulation is compared with the obtained experimentally for each of the four modes of operation selected. It can be seen that there was a very good match between them, especially at high engine loads, but also it is evident a slight tendency of the simulation to overestimate the pressure, however, the peak of the curve is very similar in the four modes of operation analyzed. The differences obtained can be attributed to the fact that the simulation did not consider the blowby and disarrangements in the model of heat transfer to the walls.

In the same way, in Figure 4, the simulated pressure profile for the four cases considered are compared and it can be seen how the pressure inside the combustion chamber increases with the engine load, according to the increase in the amount of fuel injected in response to the greater amount of energy that must be provided. This implies an advance of the start of combustion with the increase in engine load, which can be interpreted as the point at which pressure profile changes in slope close to the top dead center.

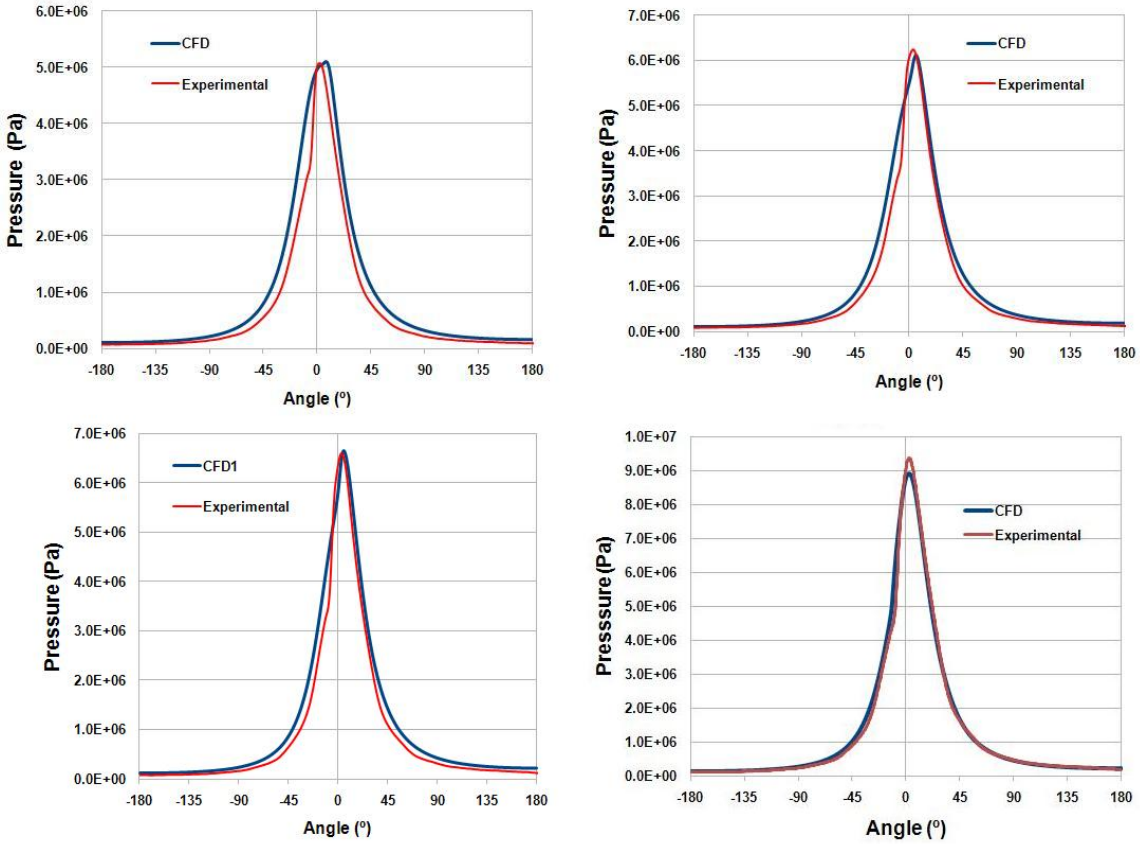

Figure 3. Variation of pressure, simulated and experimental, inside the combustion chamber, at 20 Nm upper left, at 40 Nm upper right, at 60 Nm bottom left and at 80 Nm bottom right

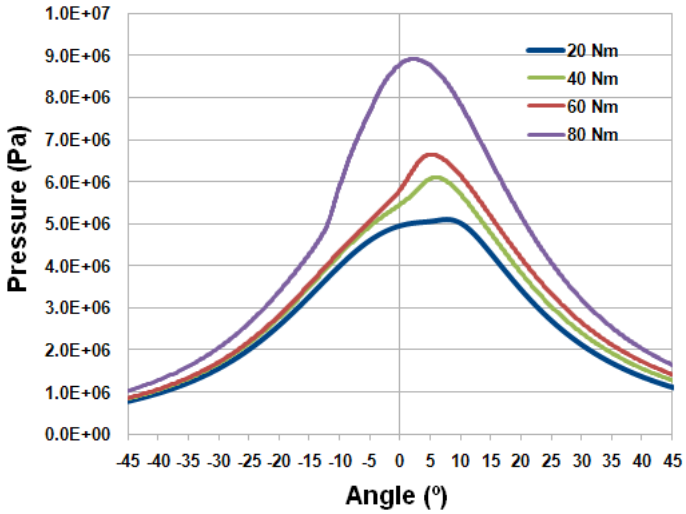

Figure 4. Comparison of pressure profiles obtained with the CFD simulation

Temperature inside the combustion chamber gives a first idea of how the exothermic reactions are developing and how the peak values are eventually influencing the formation of pollutant species such as nitrogen oxides. Figure 5 shows the spatial averaged evolution of temperature inside the chamber for the four engine load analyzed. As well as with the pressure profile, the average temperature increases with the engine load, resulting in a peak of about 1500 K for the most severe operating condition, but it must be highlighted the fact that this is an spatial averaged value and the actual temperature distribution inside the combustion chamber can achieve values near to the adiabatic flame temperature, as shown below in Figure 14. Again in Figure 5, it can be observed a change in the slope of the curve, just when the fuel injection and the subsequent processes leading to ignition and combustion have started, in such way that the discontinuity in the temperature profile occurs first at greater load, accounting for an earlier start of combustion because there is a greater amount of fuel to be burned, at the same engine speed, compared to the other engine loads. Another aspect to note is that in the case of 80 Nm load; the temperature curve during the expansion stroke experienced a change more pronounced than in the other cases examined, probably because the temperature difference with the walls was higher and therefore the rate of heat dissipation too.

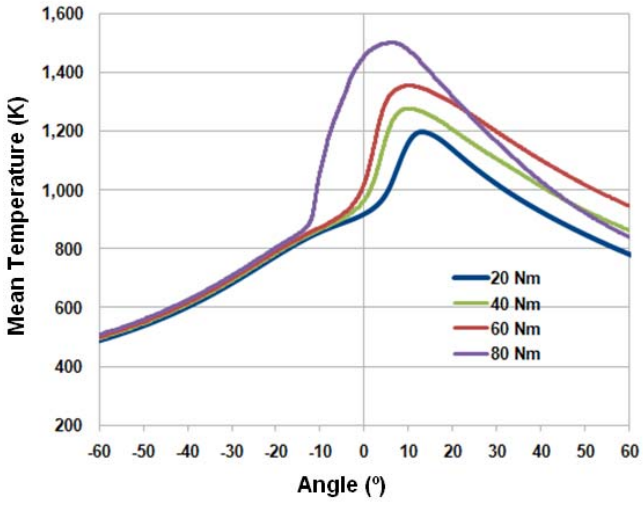

Figure 5. Comparison of temperature profiles obtained with the CFD simulation

The heat release rate (HRR) measures the rate at which heat from combustion is being released into the combustion chamber and indicates how much of this heat is released during the premixed combustion phase and how much is released into the diffusion combustion phase. Figure 6 shows the four heat release curves obtained by numerical simulation, and it can be seen how the amount of heat released increases with the engine load, because as mentioned above, it has been injected a greater amount of fuel and eventually there is a greater amount of energy stored in the fuel. At 80 Nm load, it was obtained the higher peak of heat release by premixed combustion, but at 60 Nm load was located the highest peak of heat release by diffusion combustion, which can be interpreted as at 80 Nm load the fraction of fuel burned is greater during the premixed phase than in diffusion phase, compared with the case of 60 Nm load. Also it can be observed that the delay time is virtually the same regardless of the degree of load on the engine.

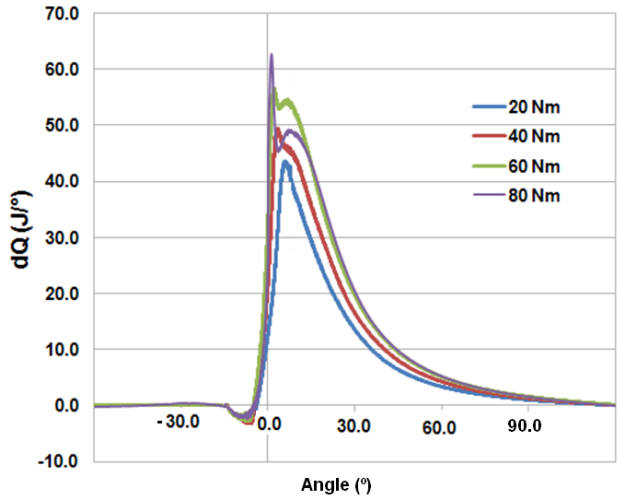

Figure 6. Comparison of heat release rates profiles obtained with the CFD simulation

Next in Figures 7 to 9 are presented the evolution inside the combustion chamber, of gaseous emissions produced during combustion for each of the four scenarios analyzed. As expected, the production of CO in diesel engines was negligible due to low or almost zero

values that were obtained, due to the excess of air which this kind of engines operate, reaching a peak of almost 200 ppm in the grater engine load, but as the same in the other modes tending to zero during the expansion stroke, this will surely be the concentration measured in the exhaust pipe.

The emission of NO deserves special attention for being one of the pollutants which is paying more attention in the challenge of diminish its production in the engine. Figure 7 shows that the production of NO (nitric oxide) increases with the engine load, presenting a sudden growth after combustion has begun to reach its higher peak, probably due to the peak release premix heat, and then decreases more slowly during the expansion stroke and stabilize almost to the beginning of the exhaust stroke. As the most influential NO formation mechanism is the thermal [11], it is reasonable that the bigger production of this pollutant occurs in the mode of 80 Nm load, and precisely in the angular interval where the higher mean temperature, of about 1500 K, was obtained (Figure 4), emitting little more than 1700 ppm. It is also noted that the production of NO appears first on the case of 80 Nm load and last in the mode of 20 Nm load, corresponding to the point where the respective average temperature curve reaches a value of about 1200 K. Notwithstanding the higher concentrations of NO were obtained when the temperature peaks occurred before, during the expansion stroke, being the location of the peak of the same order as the start of combustion, in the four cases analyzed.

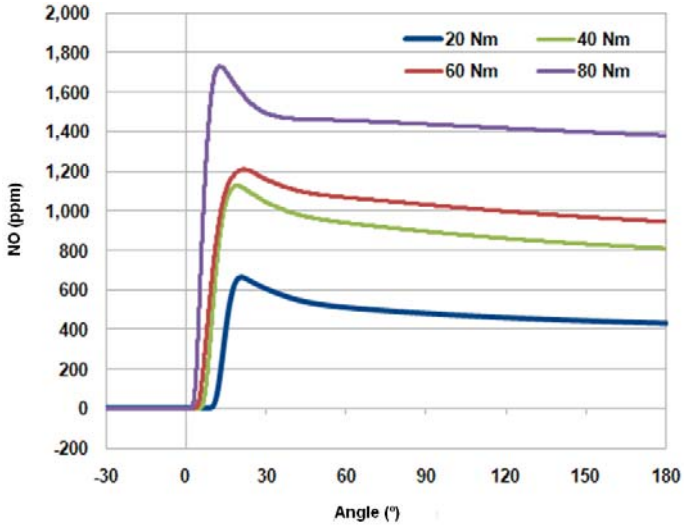

Figura 7. Comparación de la emisión de NO obtenidas con la simulación CFD, para las cuatro condiciones ensayadas

In the other hand, the emissions of CO_2 and O_2 (Figures 8 and 9) are in concordance with the well known mechanism of oxidation of fuel carbon with the oxygen present in the air, in such way that the simulated concentrations for both emissions are almost the corresponding to the stoichiometry of the combustion of n-heptane and the final values in the profile are practically the same measured for each emission. It can be observed that the velocity at which the reaction occurs is higher in the same angular interval during combustion take place, namely nearby of top dead center. The biggest emission of CO_2 was obtained at 80 Nm load and it can be explained because in this case was injected the biggest amount of fuel, and thus the difference between the emission and injected mass is proportionally the same.

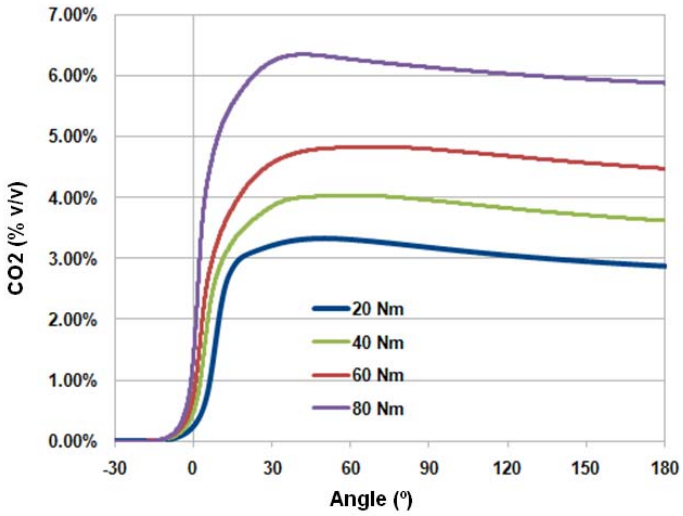

Figure 8. Comparison of the emission of CO_2 obtained with the CFD simulation, for the four cases considered

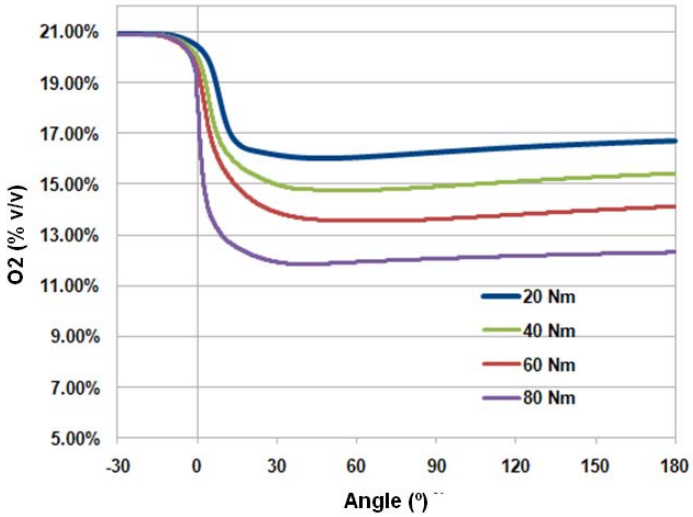

Figure 9. Comparison of the emission of O_2 obtained with the CFD simulation, for the four cases considered

Figures 10 to 12 show the comparison of emission values measured experimentally and those obtained with numerical simulation, taken as those in which the curve tends to stabilize in each of the simulated emission. Except for the case of the O_2 emission, the general trend of the simulation was to underestimate the emission in all the cases analyzed, being greater the difference in the CO_2 emissions at 40 Nm and 60 Nm load and the NO

emission at 80 Nm load. Notwithstanding the foregoing, and according to the technical details of the instrumentation used to measure tailpipe emissions, the differences obtained are similar to the respective errors and uncertainties in the measure of each species.

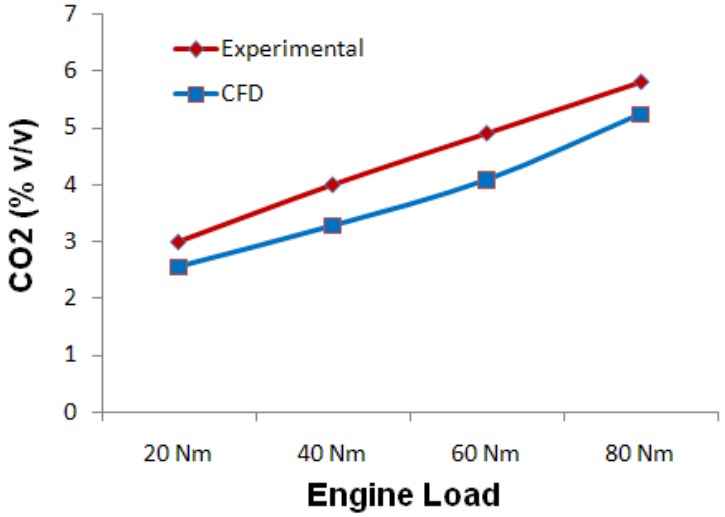

Figure 10. Comparison of the emission of CO_2 obtained with the simulation and the measured in the tailpipe of the engine

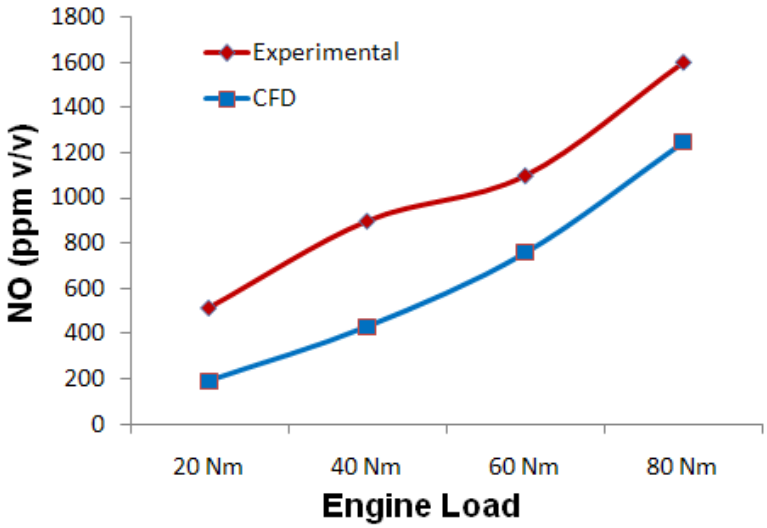

Figure 11. Comparison of the emission of NO obtained with the simulation and the measured in the tailpipe of the engine

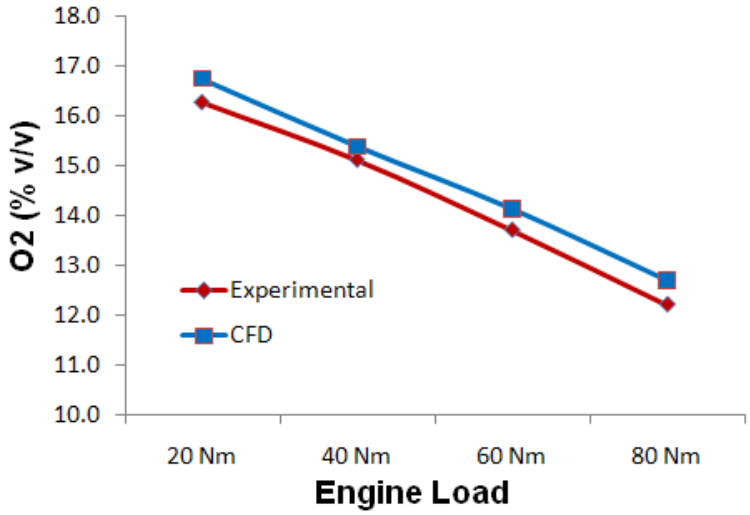

Figure 12. Comparison of the emission of O_2 obtained with the simulation and the measured in the tailpipe of the engine

Taking advantage of the nature of the solution of the tools based on CFD simulation, in Figures 13 to 16 are showed the spatial distributions inside the combustion chamber of the formation of NO, the absolute temperature, the formation of molecular oxygen and molecular nitrogen, all of them in volume fraction. The color maps correspond to a cutting plane passing through the center of the injector, splitting the chamber exactly in two equal parts, for different characteristic angles, some before the start of combustion and others when already expansion stroke has begun.

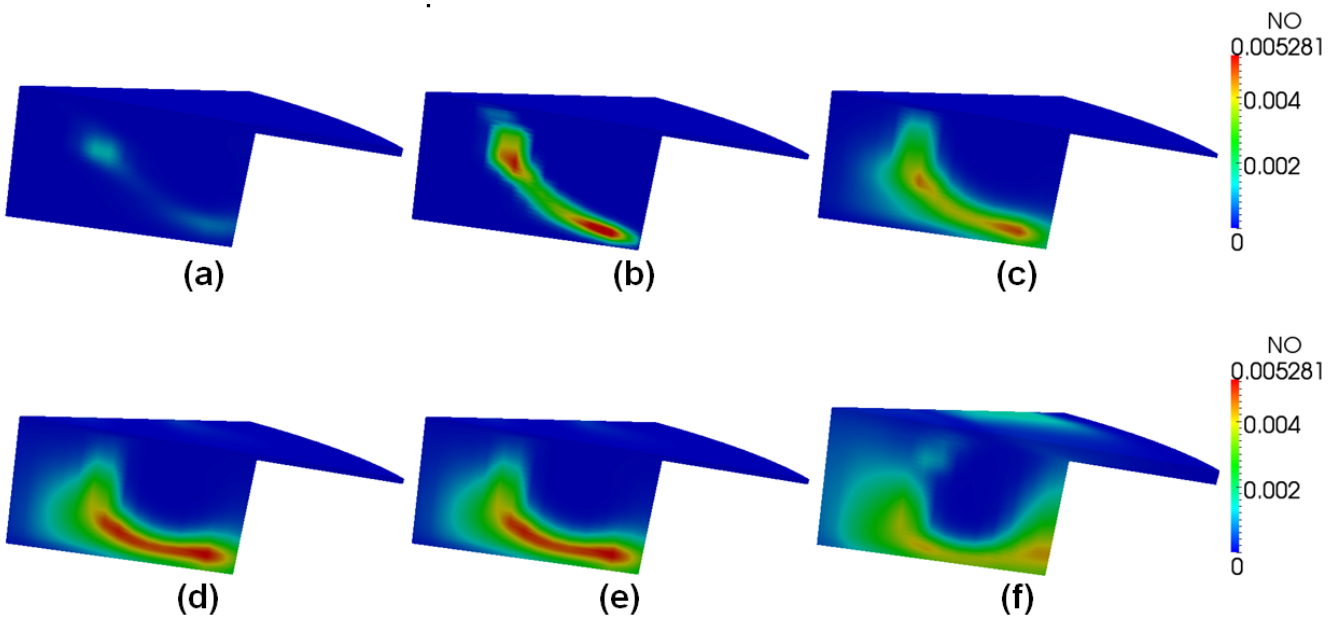

Figure 13. Temporal evolution of NO fraction inside the combustion chamber, for -8 º (a), -4º (b), 0º (c), 4º (d), 8º (e) y 12º (f)

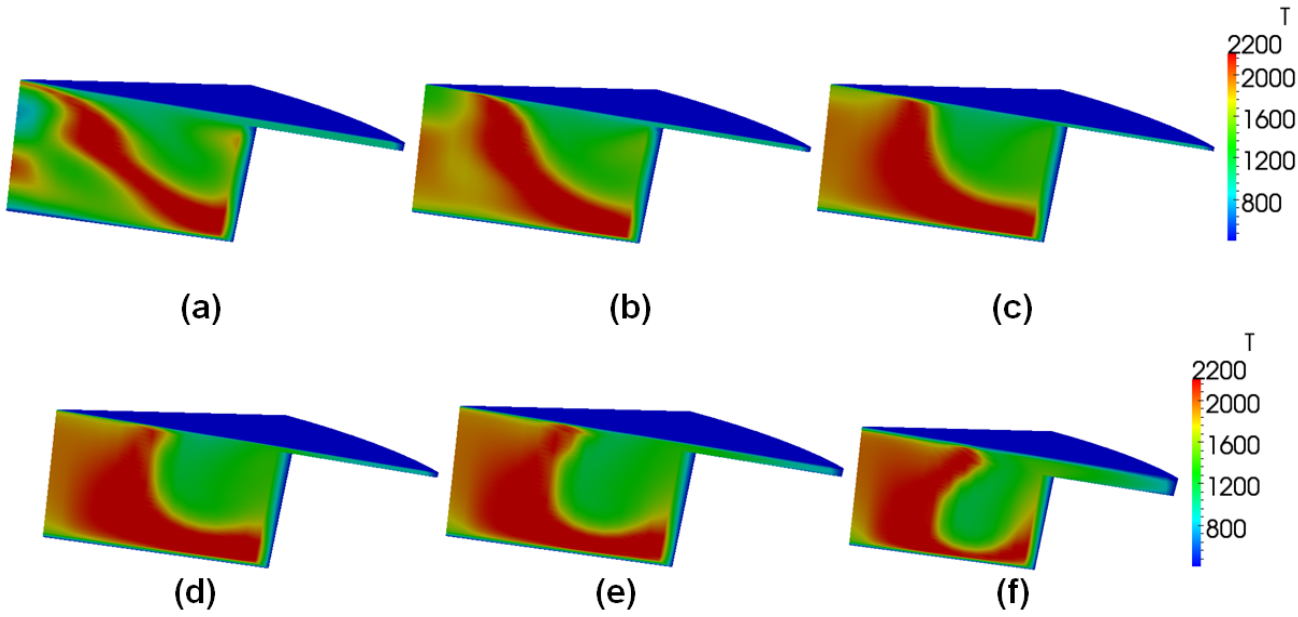

Figure 14. Temporal evolution of absolute temperature inside the combustion chamber, for -8 º (a), -4º (b), 0º (c), 4º (d), 8º (e) y 12º (f)

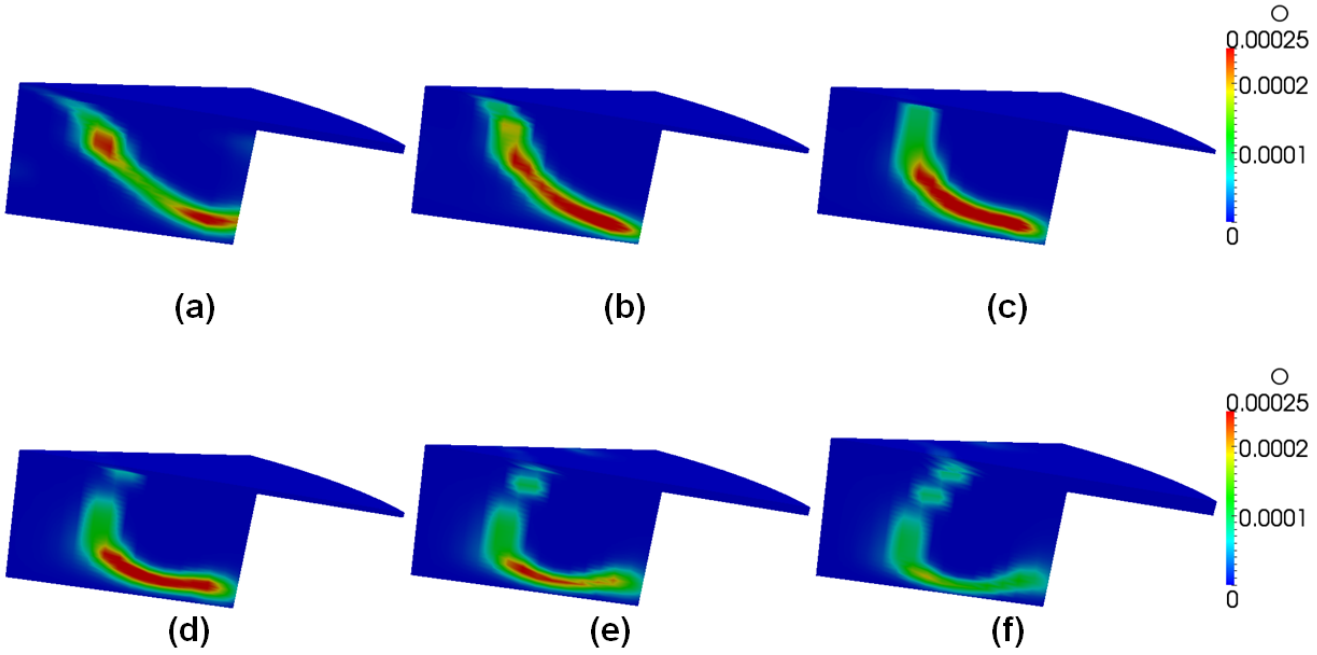

Figure 15. Temporal evolution of molecular oxygen fraction inside the combustion chamber, for -8 º (a), -4º (b), 0º (c), 4º (d), 8º (e) y 12º (f)

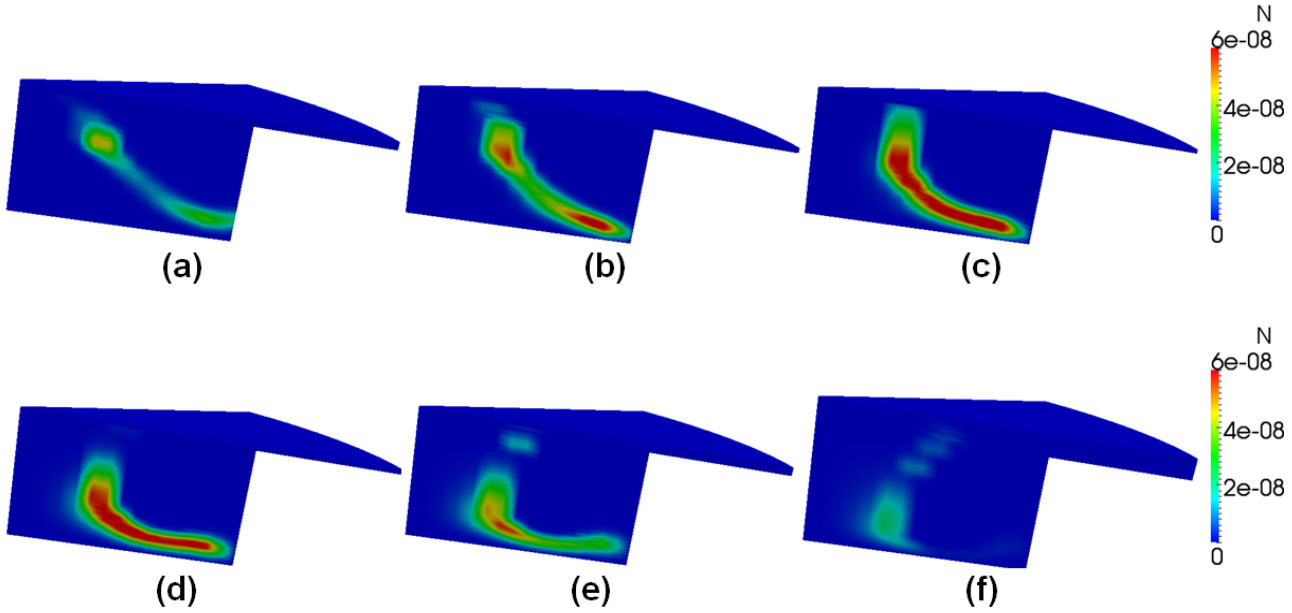

Figure 16. Temporal evolution of molecular nitrogen fraction inside the combustion chamber, for -8 º (a), -4º (b), 0º (c), 4º (d), 8º (e) y 12º (f)

Because of the angle with the horizontal which the fuel is injected inside the combustion chamber, and because of the velocity field created by the movement of the piston, the jet collides with it, spreading over its surface, resulting in zones very rich in fuel in the vicinity of the piston and zones very poor in fuel near to the cylinder head, as shown in Figures 13 and 14, where higher temperatures and NO concentrations are achieved in the vicinity of the surface of the piston, with values up 2300 K and more than 5000 ppm, respectively.

Also it is noted that NO production begins to form about 4 degrees before TDC and reaches the higher production just as the concentrations of molecular nitrogen (Fig. 16) and molecular oxygen (Figure 15) are also the largest inside the combustion chamber, which occurs in the range from 0º to 4º, which is also the range where the temperature distribution shows zones with more than 2000 K. Another detail that can be observed is that as stated Canaan and DEC [12] the areas of maximum production of NO does not necessarily coincide with those of maximum temperature inside the combustion chamber, but that occurs in areas where combustion gases reside due to the slow chemical kinetics of NO.

4.- Conclusions

In this paper it has been presented the results of a numerical simulation of combustion process in a direct injection diesel engine, for operating conditions of 2000 rpm and 20 Nm, 40 Nm, 60nm and 80 Nm load. The results consist of the typical parameters associated with combustion inside an diesel engine, such as variation in pressure and temperature inside the combustion chamber, the heat release rate and the formation of gaseous emissions. The results show that:

- For the four cases studied, were obtained profiles of average pressure inside the combustion chamber that match reasonably well to those measured on a test bench, particularly in the modes of operation of greater load, where presumably there is a greater amount of heat released. The differences may be due to mismatches in the model of heat transfer to the walls.
- The curves of heat release rate (HRR) obtained with the CFD simulation predict well the peaks of premixed and diffusion heat release, corresponding in all cases

with the zones of increased production of NOx and also the zones of highest average temperature inside the combustion chamber, despite of the relatively reduced kinetic reaction scheme employed in the simulation.

- Gaseous emissions results were quite encouraging as those predicted by the simulation correspond well with those measured in the engine tailpipe, being the magnitude of the difference equal to the uncertainty in the measurement of each species.
- In the particular case of nitrogen oxides, were obtained variations inside the combustion chamber that are comparable, both in form and magnitude, to those predicted by the theory and those obtained by other authors using reaction mechanisms even more detailed.
- With respect to emissions of CO_2 and O_2, their temporal variations were in concordance with the mechanism of oxidation of the fuel carbon for a molecule of n-heptane, so that the values estimated by simulation for the emission of CO were close to zero.
- Color maps obtained for the different variables involved in the process suggest the influence of aspects like the characteristics of injection, the combustion chamber geometry and fuel properties.
- It is necessary to perform additional simulations to establish a clear tendency about the importance of characteristic of injection on the combustion process, in order to establish a dependency with the injector orifice diameter, the fuel injection profile or the injection pressure, for example.
- Nevertheless, not only OpenFoam, but any CFD code, demonstrate the capabilities to simulate the combustion process in a diesel engine as an gasoline engine.

5.- References

[1] G. Merker, C. Schwarz, G. Stiesch, F. Otto. Simulating Combustion. Simulation of combustion and pollutant formation for engine-development. Editorial Springer. Berlín, 2004.

[2] T. Butler, L. Cloutman, J. Dukovicz, J. Conchas: An arbitrary lagrangian-eulerian computer program for multicomponent chemically reactive fluid flow at all speeds. Report LA 8929-MS, Los Alamos National Laboratory, 1979.

[3] A .Amsden, J. Ramshaw, P. O'Rourke, J. Dukovicz. Kiva: a computer program for two- and three-dimensional fluid flows with chemical reactions and fuel sprays. Report LA 10245-MS, Los Alamos National Laboratory, 1985.

[4] N. Johnson. The Legacy and Future of CFD At Los Alamos. Proceedings of the 1996 Canadian CFD Conference. Ottawa, 1996

[5] CH. Westbrook, Y. Mizobuchib, et al. Computational Combustion. Proceedings of the Combustion Institute. Volume 30, Issue 1, January 2005, Pages 125-157.

[6] S. Basha, K. Raja Gopala. In-cylinder fluid flow, turbulence and spray models—A review. Renewable and Sustainable Energy Reviews Volume 13, Issues 6-7, August-September 2009, Pages 1620-1627.

[7] N. Nordin, Complex Chemistry Model of Diesel Spray Combustion. Tesis doctoral. Chalmers University of Technology. Goteborg, 2001.

[8] E. I. Gutierrez. Modelado Numérico de la Atomización y Evaporación de un Chorro Diesel Mediante Análisis CFD. Tesis de Maestría, Universidad de Antioquia. Medellín, 2008.

[9] A. Delgado. Simulación de los procesos al interior de un motor diesel, mediante análisis CFD. Tesis de Maestría, Universidad de Antioquia. Medellín, 2010.

[10] L. Xingcai, et al. Experimental study and chemical analysis of n-heptane homogeneous charge compression ignition combustion with port injection of reaction inhibitors. Combustion and Flame. Volume 149, Issue 3, May 2007.

[11] G. Stiesch. Modeling Engine Spray and Combustion Processes. Editorial Springer. Berlín, 2005.

[12] J,E. Dec, R.E. Canaan. PLIF imaging of NO formation in a DI diesel engine. SAE Paper 980147, 1998.